Received: 15 July 2020 | Accepted: 18 November 2020

DOI: 10.1002/pamm.202000262

Framework for modelling the elastoplastic behaviour of friction welded lightweight structures under tension

Eric Heppner[1,*], **Rainer Glüge**[1], **Martin Weber**[1], and **Elmar Woschke**[1]

[1] Otto von Guericke University Magdeburg, Institute of Mechanics, PF 4120, D-39016 Magdeburg, Germany

Present-day research in the field of product development are increasingly focused on the efficient use of energy and raw material resources. In the light of this context, the design principle of consistent lightweight construction is gaining more and more importance. One possible approach is the targeted combination of different materials with favourable technological properties in hybrid structures. Against this background, the rotary friction welding (RFW), is particularly advantageous allowing the joining of dissimilar materials, like aluminium and steel in order to create such lightweight structures. The purpose of the paper at hand, is to present a framework for modelling the elastoplastic behaviour of those manufactured structures under the assumption of large deformation and non-linear material behaviour. Moreover, the presented model was implemented into a finite element analysis program (ABAQUS), in order to simulate a tensile test of a friction welded lightweight structure. Subsequently, the simulation results were critically evaluated using experimental data.

1 Introduction

The RFW process is a solid state joining technique for material bonding of two rotationally symmetric components. Therein, one part is rotating around its central axis and is pressed on the front surface of the second part under remarkable pressure to generate frictional heat. After sufficient heat was created, the movement is stopped, followed by a temporary forging stage under a higher axial pressure resulting in a sound material bond. At this point, a friction welded solid shaft hybrid structure composing of an aluminium alloy (AA 1050) and a structural steel (S355) is considered (cf. the top left of Fig. 1). It is emphasized, that the involved materials do not reach their melting temperature during the welding process. Moreover, neither any filler metal nor any auxiliary material is needed. Against this background, the heat effected zone (HAZ) is just slightly evolved in aluminium alloy, limited to an area of $2\ \mathrm{mm}$ distance from the welding interface. Concerning the steel, there was no change in microstructure observed. In order to analyse the mechanical strength a tensile test of the structure was conducted (cf. the left of Fig. 1). By means of an finite element simulation, the mechanical behaviour is computationally investigated.

2 Continuum mechanics modeling

In this section the major governing equations are presented in order to describe the framework for modelling the tensile test. First of all, it is necessary to define a decomposition assumption for the elastoplastic kinematics. As suggested in [1], a multiplicative split of the deformation gradient $\boldsymbol{F}$ is adopted:

$$\boldsymbol{F} = \boldsymbol{F}_{\mathrm{e}}\boldsymbol{F}_{\mathrm{p}}. \tag{1}$$

Therein, $\boldsymbol{F}_{\mathrm{e}}$ denotes the elastic part of the deformation gradient and $\boldsymbol{F}_{\mathrm{p}}$ is the plastic part representing an unstressed intermediate configuration. Due to the multiplicative split, the velocity gradient $\boldsymbol{L}$ evolve to:

$$\boldsymbol{L} = \dot{\boldsymbol{F}}\boldsymbol{F}^{-1} = \dot{\boldsymbol{F}}_{\mathrm{e}}\boldsymbol{F}_{\mathrm{e}}^{-1} + \boldsymbol{F}_{\mathrm{e}}\dot{\boldsymbol{F}}_{\mathrm{p}}\boldsymbol{F}_{\mathrm{p}}^{-1}\boldsymbol{F}_{\mathrm{e}}^{-1}. \tag{2}$$

For this reason, by means of the CAUCHY stress tensor $\boldsymbol{T}$ and the density ρ, the stress power l can be introduced:

$$l = {}^{1}\!/\!_{\rho}\boldsymbol{T} : \dot{\boldsymbol{F}}_{\mathrm{e}}\boldsymbol{F}_{\mathrm{e}}^{-1} + {}^{1}\!/\!_{\rho}\boldsymbol{T} : \boldsymbol{F}_{\mathrm{e}}\dot{\boldsymbol{F}}_{\mathrm{p}}\boldsymbol{F}_{\mathrm{p}}^{-1}\boldsymbol{F}_{\mathrm{e}}^{-1}. \tag{3}$$

The first term reveals the temporal change of the elastic energy $\dot{w}$ whereas the second one accounts the plastic dissipation. Moreover, for the elastic term holds the relation:

$$\dot{w} = \frac{\partial w}{\partial t} = \frac{\partial w}{\partial \boldsymbol{F}_{\mathrm{e}}} : \dot{\boldsymbol{F}}_{\mathrm{e}} = \frac{\partial w}{\partial \boldsymbol{F}_{\mathrm{e}}}\boldsymbol{F}_{\mathrm{e}}^{T} : \dot{\boldsymbol{F}}_{\mathrm{e}}\boldsymbol{F}_{\mathrm{e}}^{-1}. \tag{4}$$

The elastic law can be identified by comparing the coefficients of the first term of Eq. (3) and the last part of Eq. (4). Finally, it follows:

$$\boldsymbol{T} = \rho\frac{\partial w}{\partial \boldsymbol{F}_{\mathrm{e}}}\boldsymbol{F}_{\mathrm{e}}^{T}. \tag{5}$$

* Corresponding author: e-mail eric.heppner@ovgu.de, phone +49 391 67 57178, fax +49 391 67 12439

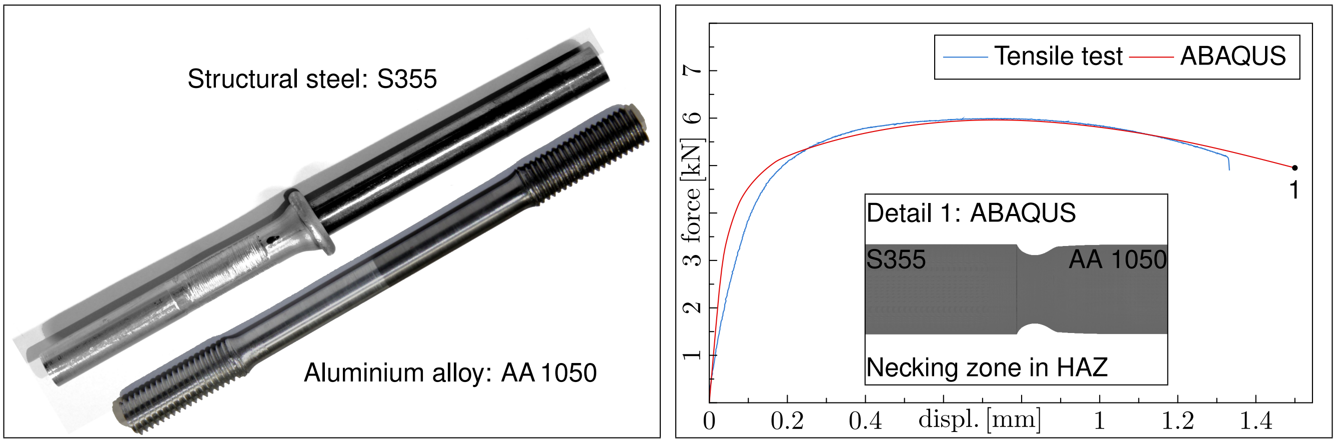

Fig. 1: Friction welded hybrid structure and tensile test specimen (left), experiment vs. simulation (right)

With respect to the considered materials, the SAINT VERNANT-KIRCHHOFF elastic energy formulation was adopted [1]:

$$w = {}^{\lambda}\!/_{2}\big(\mathrm{tr}(\boldsymbol{E})\big)^2 + \mu\,\mathrm{tr}\big(\boldsymbol{E}^2\big). \tag{6}$$

Therefore, the LAMÉ parameters λ and μ as well as the GREEN-LAGRANGE strain $\boldsymbol{E}$ were taken into account:

$$\boldsymbol{E} = {}^{1}\!/_{2}\left(\boldsymbol{F}_{\mathrm{e}}^{T}\boldsymbol{F}_{\mathrm{e}} - \boldsymbol{I}\right). \tag{7}$$

Next, the yield criteria ϕ, being an indicator function for the plastic flow, is defined in terms of the deviatoric part of the CAUCHY stress tensor $\boldsymbol{T}'$ and a critical yield stress value σ_{y} [1]:

$$\phi = \sqrt{{}^{3}\!/_{2}\boldsymbol{T}' : \boldsymbol{T}'} - \sigma_{\mathrm{y}}. \tag{8}$$

In case of $\phi < 0$, the deformation process is only elastic and $\dot{\boldsymbol{F}}_{\mathrm{p}} = 0$. However, if $\phi = 0$ and $\dot{\phi}|_{\boldsymbol{F}_{\mathrm{p}}=\mathrm{con}} > 0$, the deformation is elastoplastic. In addition, $\dot{\boldsymbol{F}}_{\mathrm{p}} > 0$ must be valid. The critical yield stress value evolves by a VOCE-type hardening law [1]:

$$\dot{\sigma}_{\mathrm{y}} = K\left(\sigma_{\star} - \sigma_{\mathrm{y}}\right)\dot{\xi}, \tag{9}$$

including the material parameters K and $\sigma_{\star}$, which need to be determined experientially. The internal variable is given by:

$$\dot{\xi} = \sqrt{{}^{2}\!/_{3}}\gamma, \tag{10}$$

in terms of the plastic strain rate γ [2]. In the rate-independent plasticity case, the plastic strain rate has the character of a LAGRANGE multiplier for the plastic flow and is estimated by the flow rule. Finally, the flow rule can be obtained by the plastic dissipation power. Considering the principle of maximum of plastic dissipation, the plastic dissipation (cf. second part of Eq. (3)) is maximal if $\boldsymbol{T}$ is parallel to $\boldsymbol{F}_{\mathrm{e}}\dot{\boldsymbol{F}}_{\mathrm{p}}\boldsymbol{F}_{\mathrm{p}}^{-1}\boldsymbol{F}_{\mathrm{e}}^{-1}$. Hence, the flow rule is specified by:

$$\dot{\boldsymbol{F}}_{\mathrm{p}}\boldsymbol{F}_{\mathrm{p}}^{-1} = \gamma\frac{1}{\rho}\left(\boldsymbol{F}_{\mathrm{e}}^{-1}\frac{\boldsymbol{T}}{|\boldsymbol{T}|}\boldsymbol{F}_{\mathrm{e}}\right)' = \gamma\frac{1}{\rho}\boldsymbol{F}_{\mathrm{e}}^{-1}\frac{\boldsymbol{T}'}{|\boldsymbol{T}'|}\boldsymbol{F}_{\mathrm{e}}. \tag{11}$$

It is underlined, that only volume preserving plasticity and isotropic elasticity is assumed. Furthermore, only the symmetric part of the $\dot{\boldsymbol{F}}_{\mathrm{p}}\boldsymbol{F}_{\mathrm{p}}^{-1}$ is considered, since skew symmetry part describes a rotation of the unstressed intermediate configuration which does not affect the elastic law due to the presumption of isotropy. In the last consequence, it is set that:

$$\left(\dot{\boldsymbol{F}}_{\mathrm{p}}\boldsymbol{F}_{\mathrm{p}}^{-1}\right)_{\mathrm{skw}} = 0. \tag{12}$$

The presented model was implemented in ABAQUS via a user material subroutine [3], in order to demonstrate the applicability concerning the simulation of tensile tests. Note that the geometry as well as the realistic boundary conditions are taken into account. The right of Fig. 1 compares the simulated and the experimentally measured force-displacement curve.

Acknowledgements Open access funding enabled and organized by Projekt DEAL.

References

[1] A. Bertram, Elasticity and Plasticity of Large Deformations: An Introduction (Springer-Verlag Berlin Heidelberg, Berlin, Heidelberg, 2012), p. 296.
[2] H. Parisch, Festkörper-Kontinuumsmechanik (Vieweg+Teubner Verlag, Wiesbaden, 2003), p. 188.
[3] Abaqus 2017 Documentation (Dassault Systemes, 2017).

